ADMET & DMPK **14** (2026) 3608*; doi: https://doi.org/10.5599/admet.3608*

ADMET

Open Access : ISSN : 1848-7718

http://www.pub.iapchem.org/ojs/index.php/admet

Original scientific paper

An electrochemical platform for determination of epinine based on a glassy carbon electrode modified with hematoxylin and MoS_2 nanosheets

Rawaa Abdulmutalib[1], Noor Mahmood Mahdi[2], Hussein Ali Al-Bahrani[3], Mustafa Mudhafar[4,*] and Hasan Ali Alsailawi[5]

[1]*Department of Chemistry, College of Science, University of Thi-Qar, Iraq*
[2]*Department of Basic Sciences, College of Dentistry, University of Kerbala, Karbala, 56001, Iraq*
[3]*College of Nursing, University of Al-Ameed, Department of Chemistry, Collage of Education for Pure Science, University of Kerbala, Iraq*
[4]*Centre for Research on Environment and Renewable Energy, University of Kerbala, Karbala, 56001, Iraq and Department of Therapeutic Nutrition Technologies, Al Taff University College, 56001, Kerbala, Iraq (Almosawy2014@gmail.com)*
[5]*Department of Basic Sciences, College of Dentistry, University of Kerbala, 56001, Karbala, Iraq*

Corresponding Author: E-mail: *almosawy2014@gmail.com*

Received: July 3, 2026; Revised: September 3, 2026; Published: October 26, 2026

Abstract

Background and purpose: Epinine (EPN) is a catecholamine with a pharmacological profile similar to that of epinephrine. Excessive use of EPN can have harmful effects in humans and must be used cautiously. **Experimental approach:** A unique glassy carbon electrode was created using MoS_2 nanosheets and hematoxylin (HX/MoS_2 Ns/GCE). This article describes the electrochemical analysis of the HX/MoS_2 Ns/GCE in the oxidation of EPN. **Key results:** The oxidation of EPN occurs about 310 mV less positive. Using differential pulse voltammetry, the detection limit for EPN was determined to be 0.4 µM. **Conclusion:** The modified electrode was employed to measure the EPN in urine and tap water samples.

©2026 by the authors. This article is an open-access article distributed under the terms and conditions of the Creative Commons Attribution license (http://creativecommons.org/licenses/by/4.0/).

Keywords

N-methyldopamine, deoxyepinephrine, transition metal dichalcogenides; modified electrodes

Introduction

Glassy carbon electrodes (GCE) are often used for electroanalytical applications because they are mechanically robust, operate over a broad potential range, exhibit low background current, and resist chemicals well. Still, when people use bare GCEs, they often encounter poor sensitivity, weak selectivity, and surface fouling [1]. This usually comes from slow electron-transfer kinetics and weak adsorption of the analytes onto the electrode surface. To address this, researchers have modified bare electrodes with suitable redox-active to shape and improve electrochemical sensors. In real lab work, surface modification is also used to reduce overvoltage and address sluggish kinetics in many electrode reactions [2,3].

One flavonoid compound, hematoxylin (HX), is derived from catechol [4]. The electrochemical characteristics of HX-modified electrodes and their use as biosensors to identify ascorbic acid, NADH, uric acid, and adrenaline have recently guided certain researchers [5]. These findings demonstrate that HX is an effective redox mediator for the electrocatalysis of significant biological molecules [6].

In recent years, two-dimensional ultra-thin materials have gained growing interest due to their outstanding properties and, more significantly, their technological potential, ranging from environment-related applications such as energy storage to biomedical and biological directions, such as drug carriers, catalysts, semiconductors, sensors, and personal care products [7]. Two-dimensional transition metal dichalcogenides (2D-TDMs), especially 2D-MoS_2 nanosheets, have become increasingly important as they are one of the most utilized two-dimensional materials, owing to the existence of a large band gap that changes from indirect to direct upon moving towards single layers, along with their remarkable catalytic and electrocatalytic activity [8]. In electrochemistry, electrochemical sensing of electroactive biomolecules is essential for biomedical applications, and its deployment is expanding rapidly [9]. As with graphene [10], the feasibility of using two-dimensional MoS_2 as an efficient material for electroactive biomolecule sensing [11] has already been proven.

Deoxyepinephrine, or epinine (EPN), commonly referred to as N-methyldopamine, is a catecholamine and an endobiotic compound widely present in plants, animals, and insects, with a pharmacological profile similar to that of epinephrine. It can be prepared by enzymatic hydrolysis of the cardiovascular drug ibopamine, which is used to treat congestive heart failure [12]. Although Barger and Dale observed a pressor response to EPN in vivo, which indicates it is either a pressor itself or close to a pressor, the excessive use of EPN has potential ill effects on human beings due to its manifold virtues and, as a result, must be applied cautiously [13-16].

The manufacture and applicability of MoS_2 nanosheets and hematoxylin-modified GCE (HX/MoS_2 Ns/GCE) as well as the measurement of EPN, are now being reported for the first time. The improved electrode's analytical performance in measuring HX/MoS_2 Ns/GCE is next tested on actual samples.

Experimental

Apparatus and chemicals

PGSTAT 12 N (the Netherlands) was used to conduct the electrochemical measurements. The reference, auxiliary, and working electrodes were an Ag/AgCl/KCl electrode, a platinum wire, and the HX/MoS_2 Ns/GCE. Merck (Germany) provided EPN, HX and all other analytical-grade reagents. Phosphoric acid and its salts were used to make the buffer solutions (pH 2.0 to 9.0).

Synthesis of MoS_2 nanosheets

Initially, 35 mL of DI water was mixed with 0.4110 g of thiourea (5.40 mmol) and stirred for 10 min at room temperature to dissolve it completely. Next, while stirring, 0.2224 g of $(NH_4)_6Mo_7O_{24}{\cdot}4H_2O$ (0.18 mmol) was added. The solution was stirred magnetically for one hour. The combined mixture was then placed in an autoclave and heated to 200 °C for 15 h. The precipitates formed at the bottom of the autoclave were then collected, repeatedly washed with ethanol, and dried for 15 hours at 67 °C.

Preparation of modified glassy carbon electrodes

The GCE surface was drop-cast with 4 µL of MoS_2 Ns (1 mg / 1 mL). Finally, HX/MoS_2 Ns/GCE was fabricated by immersing the MoS_2 Ns-modified GCE in phosphate buffer solution (PBS) containing 0.1 M HX. Then, the obtained HX/MoS_2 Ns/GCE was further adjusted by scanning between -0.4 and 0.5 V at 100 mV s^{-1}. For fabricating the HX-modified GCE (HX/GCE), GCE was immersed in PBS containing 0.1 M HX and modified in exactly the same manner described for HX/GCE.

Real samples preparation

Fresh urine was centrifuged immediately after sampling at 1500 rpm for 10 min and varying aliquots were prepared by dilution with PBS. Different amounts of EPN were spiked into this diluted urine sample solution.

(cc) BY

Simultaneously, a tap water sample was obtained, filtered through a membrane filter, and added to PBS. Finally, the proposed method was used to determine EPN contents in the water samples.

Results and discussion

Electrochemical properties of MoS_2 nanosheets and hematoxylin-modified glassy carbon electrode

Cyclic voltammetry (CV) was performed to synthesize HX/MoS_2 Ns/GCE and test the electrochemical behaviour of HX/MoS_2 Ns/GCE in PBS. The results showed anodic and cathodic peak potentials (E_{pa} = 190 mV and E_{pa} = 150mV).

Electrocatalytic oxidation of epinine at MoS_2 nanosheets and hematoxylin-modified glassy carbon electrode

CV curves of 30.0 µM EPN with different electrode materials are depicted in Figure 1.

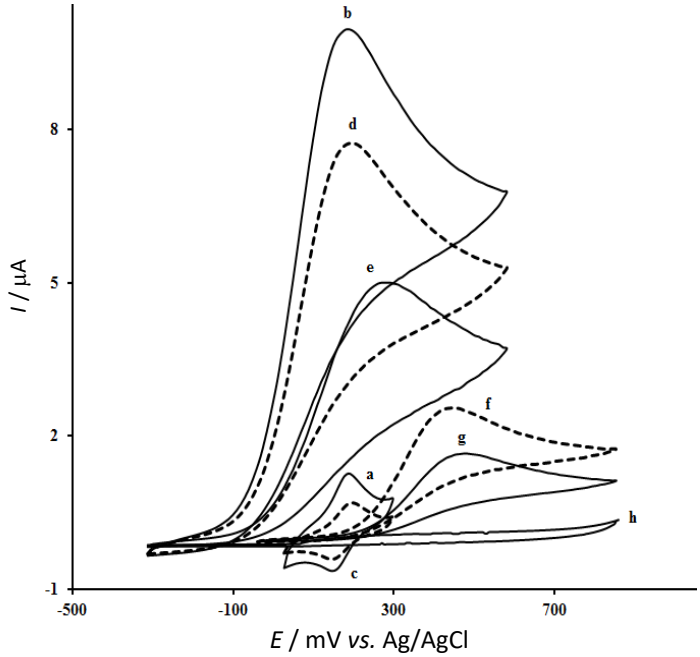


Figure 1. CVs of HX/MoS_2 Ns/GCE in PBS at a scan rate of 10 mV s^{-1}, in the absence (a) and presence of 30.0 µM EPN (b). (c) like (a) and (d) like (b) for an HX/GCE. (e-g) like (b) for the activated MoS_2 Ns-modified electrode, and then bare GCE, and finally (h) like (a) for bare GCE

The oxidation potential at HX/MoS_2 Ns/GCE and HX/GCE is located around 190 mV. For activated GCE (curve e), it is around 290 mV; for MoS_2 Ns-modified GCE (curve f), it is around 445 mV; and for bare GCE (curve g), it is around 500 mV.

A distinct anodic peak can be found for MoS_2 Ns-modified GCE and activated GCE, but the oxidation potentials are higher than the peak potentials obtained at HX/MoS_2 Ns/GCE and HX/GCE. Hence, the HX/MoS_2 Ns/GCE exhibits better electrocatalytic performance. In PBS, the HX/MoS_2 Ns/GCE shows a stable and reversible redox behaviour (curve a). When 30.0 µM EPN was added to the solution, an increase in current was obtained (curve b). Otherwise, HX/GCE also showed cyclic voltammetry with a rather low current response when EPN was not in PBS (pH 7.0) (curve c). We also observe that, in HX attached to MoS2 Ns, a pair of well-behaved redox peaks is observed, compared with the bare GCE. In the porous interfacial film of MoS2 Ns-modified GCE, the mediator HX passes more readily through the electrically conducting porous channel to the electrode, thus giving higher sensitivity.

Effect of scan rate

We evaluated the effect of scan rate (v) on EPN at HX/MoS_2 Ns/GCE *via* CV (Figure 2).

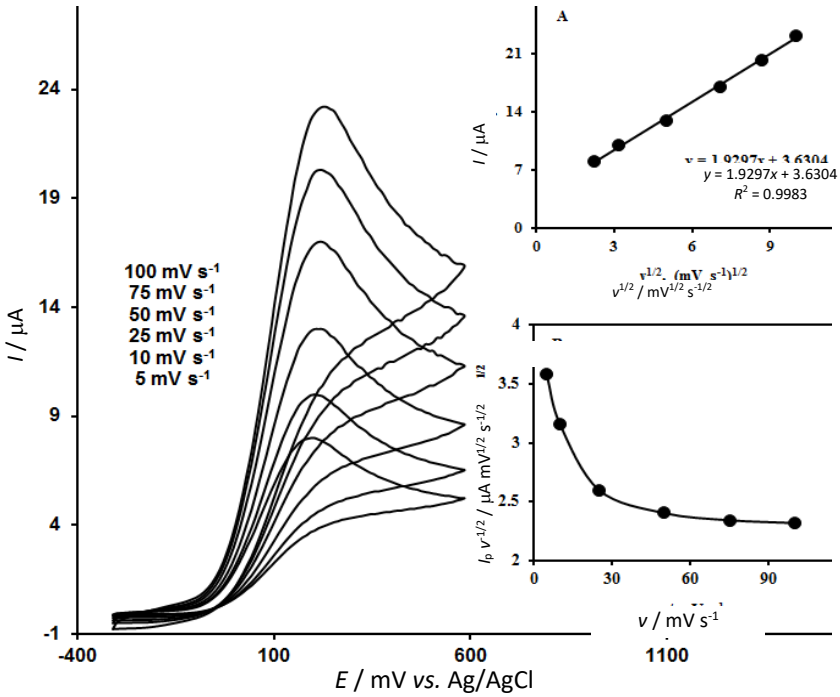


Figure 2. CVs of HX/MoS_2 Ns/GCE in PBS containing 30.0 µM EPN at different scan rates. Insets: variation of (A) *I vs.* $v^{1/2}$; and (B) normalized current ($I/v^{1/2}$) *vs. v*

Chronoamperometric measurements

Electrode processes at HX/MoS_2 Ns/GCE were investigated using chronoamperometry. Figure 3A shows the chronoamperometric data for EPN at HX/MoS_2 Ns/GCE. The current-time profiles for different EPN concentrations are shown in this figure. The Cottrell Equation (1) describes the current relation with the diffusion coefficient (*D*):

$$I = nFAD^{1/2}C\Pi^{-1/2}t^{-1/2} \quad (1)$$

where *C* / mol cm^{-3} is the concentration. *I vs.* $t^{-1/2}$ plot is linear under the diffusion-controlled condition (Figure 3B). The slopes against the EPN concentration were plotted (Figure 4A). The *D* was determined to be 1.05×10^{-5} cm^2 s^{-1}.

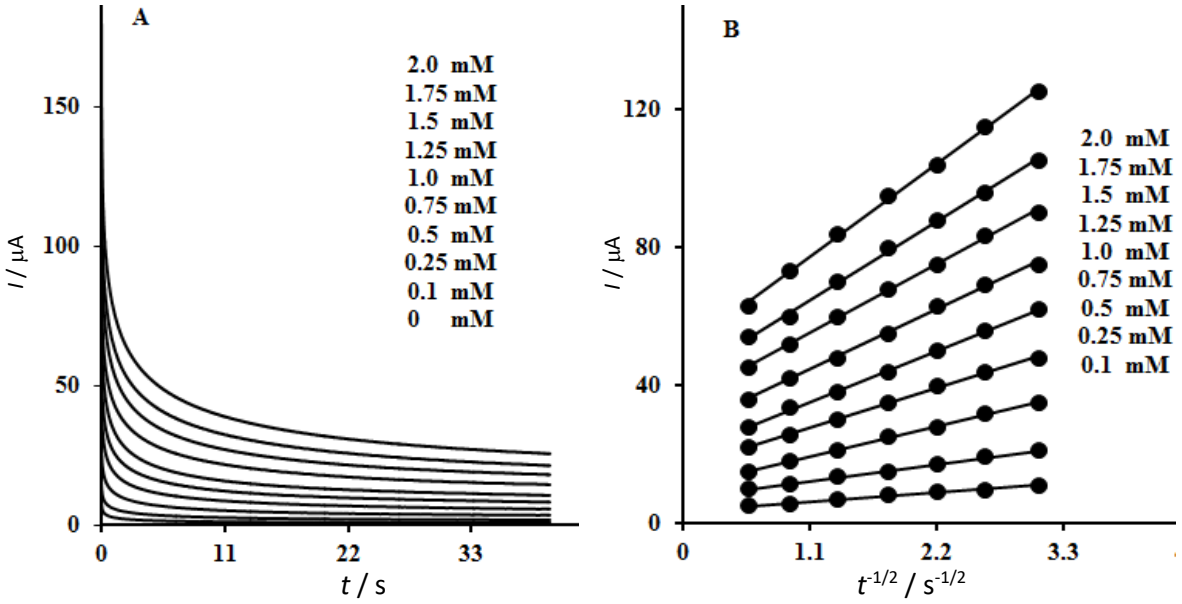


Figure 3. (A) Chronoamperograms recorded at HX/MoS_2 Ns/GCE in PBS for several EPN concentrations. (B) *I vs.* $t^{-1/2}$

CC BY

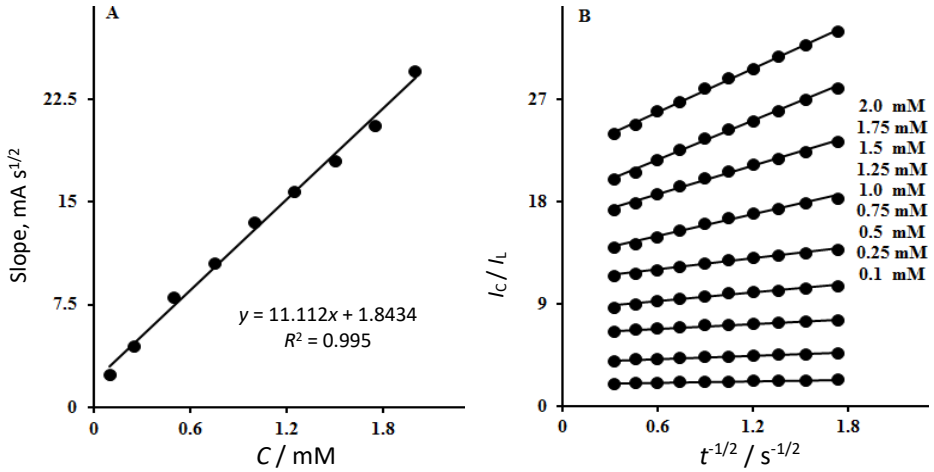


Figure 4. (A) Slope of straight lines as a function of EPN concentration. (B) The relationship of I_C / I_L with $t^{1/2}$.

The catalytic rate constant, *k*, can be determined using chronoamperometry using the Galus method [17], Equation (2):

$$I_C / I_L = \gamma^{1/2}[\pi^{1/2}\ \mathrm{erf}\ (\gamma^{1/2}) + \exp(-\gamma)/\gamma^{1/2}] \quad (2)$$

where I_C is the catalytic current of EPN, I_L is the limiting current in the absence of EPN and $\gamma = kC_bt$. In cases where $\gamma > 2$, Equation (3) applies.

$$I_C / I_L = \pi^{1/2}\gamma^{1/2} = \pi^{1/2}(kC_bt)^{1/2} \quad (3)$$

where *t* is the time elapsed in seconds. Based on the slope of the I_C / I_L *vs.* $t^{1/2}$ plot, $k = 4.09\times10^3\ M^{-1}\ s^{-1}$.

Quantitative determinations

EPN concentration was calculated using DPV (Figure 5). Two linear segments made up the plot of peak current vs. EPN concentration. The LOD was obtained 0.7 µM for EPN.

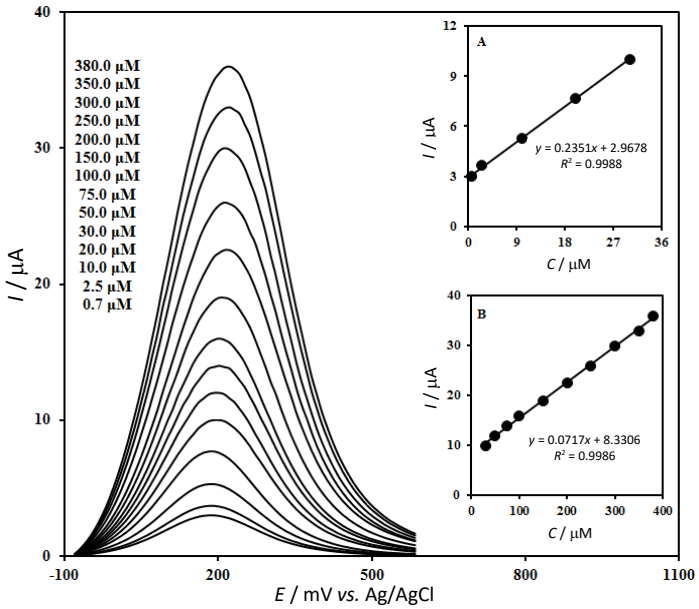


Figure 5. DPVs of HX/MoS_2 Ns/GCE in PBS(pH 7.0) containing assorted EPN levels. Insets show electrocatalytic peak current *vs.* EPN concentration: (A) 0.7 to 30.0 µM and (B) 30.0 to 380.0 µM

Real sample analysis

EPN may be successfully determined using the described approach in actual urine and water specimen samples. This investigation used the usual addition approach, and Table 1 presents the results. The ability of HX/MoS_2 Ns/GCE as a voltammetric sensor for EPN analysis in real samples was validated by the notable

recovery rates (97.5 to 103.3 %) and relative standard deviations (RSDs) (1.9 to 3.5 %). Additionally, the relative standard deviation (RSD) was used to describe the method's repeatability.

Table 1. Determination of EPN in real samples using HX/MoS_2 Ns/GCE.

Sample	Content, µM		Recovery, %	RSD, %
	Added	Found		
Urine	0	-	-	-
	5.0	4.9	98.0	3.5
	7.0	7.1	101.4	2.2
	9.0	9.3	103.3	2.8
	11.0	10.9	99.0	1.9
Tap water	0	-	-	-
	6.0	6.2	103.3	2.4
	8.0	7.8	97.5	3.0
	10.0	10.1	101.0	2.3
	12.0	11.9	99.2	2.5

Conclusions

The creation of an HX as a modifying species is demonstrated in this work. The HX/MoS_2 Ns/GCE exhibited significant stability. This electrode's detection limit and potential shifts are superior to those seen in prior studies. This electrode is straightforward to make and easy to renew. CV was used to examine the electrochemical behaviour of the HX/MoS_2 Ns/GCE with and without EPN. The findings indicate that EPN oxidation is catalysed at pH 7.0, while EPN's peak potential shifts by 310 mV at the HX/MoS_2 Ns/GCE surface.

References

[1] E. Kipkorir, O. Kimani. Electrochemical sensing of pharmaceutical pollutants using modified glassy carbon electrodes with nanostructures. *Inorganic Chemistry Communications* **179** (2025) 114827. https://doi.org/10.1016/j.inoche.2025.114827

[2] N. Mandal, R. Mitra, B. Pramanick. Bio-synthesized silver nanoparticle modified glassy carbon electrode as electrochemical biosensor for prostate specific antigen detection. *Carbon Trends* **13** (2023) 100315. https://doi.org/10.1016/j.cartre.2023.100315

[3] M. Roushani, Z. M. Karazan, Q. A. Mohammed. Electrochemical determination of lead ions in different samples using glassy carbon electrode modified with electroreduced graphene oxide and poly tryptophan in food samples. *Journal of Food Composition and Analysis* **156** (2026) 109339. https://doi.org/10.1016/j.jfca.2026.109339

[4] J. Shi, L. Liang, X. Meng, J. Wei, W. Song, B. Zhou, M. Liang, M. Du, Y. Gao. Pathomics predict CD40LG expression and clinical prognosis in lung adenocarcinoma based on haematoxylin-eosin-stained images. *Pathology - Research and Practice* **274** (2026) 156181. https://doi.org/10.1016/j.prp.2025.156181

[5] H. R. Zare, N. Nasirizadeh. Simultaneous determination of ascorbic acid, adrenaline and uric acid at a hematoxylin multi-wall carbon nanotube modified glassy carbon electrode. *Sensors and Actuators B* **143** (2010) 666-672. https://doi.org/10.1016/j.snb.2009.10.030

[6] Y. Dilgin, B. Kızılkaya, B. Ertek, F. Işık, D. Giray Dilgin. Electrocatalytic oxidation of sulphide using a pencil graphite electrode modified with hematoxylin. *Sensors and Actuators B* **171-172** (2012) 223-229. https://doi.org/10.1016/j.snb.2012.03.020

[7] J. Hu, P. Zhang, T. Yang, Y. Cai, J. Qu, X. Yang. Screen superior ultra-thin g-C_3N_4 material for photocatalytic in-situ H_2O_2 production to remove tetracycline. *Applied Surface Science* **576** (2022) 151841. https://doi.org/10.1016/j.apsusc.2021.151841

[8] M. Fang, D. Duan, Z. Liu, R. Zhu, J. Liu. Multimode Immunochromatographic Detection Technology Based on Multifunctional MoS_2@Au Nanosheets for Highly Sensitive Monkeypox Virus Detection. *Sensors and Actuators Reports* **12** (2026)100485. https://doi.org/10.1016/j.snr.2026.100485

(cc) BY

[9] S. Yeon Jung, D. Su Kim, D. Rhee, K. Woong Lee, Y. Seong Cho, A. D. Alfieri, J. Lynch, D. Jariwala, H. Koun Cho, J. Kang. Multiscale hierarchically wrinkled MoS_2 nanosheet films with enhanced photoelectrochemical properties. *Chemical Engineering Journal* **538** (2026) 176992. https://doi.org/10.1016/j.cej.2026.176992

[10] J. Ma, R. Wang, D. Li, K. Xu. MoS_2-Graphene heterostructure enhanced fiber optic SPR sensor for highly sensitive glucose detection. *Microchemical Journal* **213** (2025) 113753. https://doi.org/10.1016/j.microc.2025.113753

[11] S. Agrahari, A. Kumar Singh, I. Tiwari, S. Srikrishna. Electrochemical deposition of Pd on MoS_2 supported graphene nanoflakes over functionalised MWCNTs as an immunosensor for detection of lung cancer biomarker. *Microchemical Journal* **196** (2024) 109698. https://doi.org/10.1016/j.microc.2023.109698

[12] I. Martínez-Mir, V. Palop, F. J. Morales-Olivas, L. Estañ, E. Rubio. The Effects of Epinine on Arterial Blood Pressure and Regional Vascular Resistances in Anesthetized Rats. *General Pharmacology: The Vascular System* **31** (1998) 75-79. https://doi.org/10.1016/S0306-3623(97)00447-3

[13] G. Barger, HH. Dale, Chemical structure and sympathomimetic action of amines, *The Journal of Physiology* **41** (1910) 19-59. https://doi.org/10.1113/jphysiol.1910.sp001392

[14] F. Boomsma, G. Alberts, F. A. J. van der Hoorn, A. J. Man in 't Veld, M. A. D. H. Schalekamp. Simultaneous determination of free catecholamines and epinine and estimation of total epinine and dopamine in plasma and urine by high-performance liquid chromatography with fluorimetric detection. *Journal of Chromatography B* **574** (1992) 109-117. https://doi.org/10.1016/0378-4347(92)80104-X

[15] S. Z. Mohammadi, S. Tajik, Y. Badri. A voltammetric epinine sensor based on MWCNTs/ZnCo-ZIF nanocomposite and ionic liquid modified electrode. *Journal of Materials Science: Materials in Electronics* **35** (2024) 201. https://doi.org/10.1007/s10854-024-11926-9

[16] R. Zainul, A. N. M. Ansori. Voltammetric sensor for epinine determination based on ferrocene-modified carbon paste electrode. *Journal of Environmental and Bioanalytical Electrochemistry* **1** (2025) 24-32. https://doi.org/10.48309/jebe.2025.499046.1004

[17] Z. Galus, Fundamentals of Electrochemical Analysis, Ellis Horwood, New York,1976. ISBN 978-047015-080-1

©2026 by the authors; licensee IAPC, Zagreb, Croatia. This article is an open-access article distributed under the terms and conditions of the Creative Commons Attribution license (http://creativecommons.org/licenses/by/4.0/)